Heliyon 10 (2024) e39390

Contents lists available at ScienceDirect

Heliyon

journal homepage: www.cell.com/heliyon

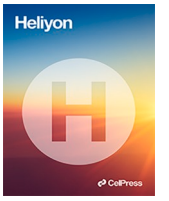

Research article

Anemarrhena asphodeloides Bunge polysaccharides alleviate lipoteichoic acid-induced lung inflammation and modulate gut microbiota in mice

Yuqi Wen [a,1], Hidayat Ullah [a,1], Renzhen Ma [a], Nabeel Ahmad Farooqui [a], Jiaxin Li [a], Yamina Alioui [a], Juanjuan Qiu [b,*]

[a] *Department of Biotechnology, College of Basic Medical Science, Dalian Medical University, Dalian 116044, China*
[b] *Central Lab, The First Affiliated Hospital of Dalian Medical University, Dalian, China*

ARTICLE INFO

Keywords:
Pneumonia. lipoteichoic acid
Gut microbiota
Anemarrhena asphodeloides

ABSTRACT

Pneumonia remains a prevalent infection primary ailment characterized by severe lung inflammation, leading to respiratory distress and significant mortality rates, particularly affecting young children in less developed regions. This study explores the therapeutic potential of low and high-molecular weight polysaccharides derived from *Anemarrhena asphodeloides* in a murine model of lipoteichoic acid (LTA)-induced pneumonia, which represents bacterial-induced lung inflammation. Administration of *Anemarrhena asphodeloides* polysaccharides effectively alleviated LTA-induced symptoms, including decreased lung and colon inflammation, and restored dysbiosis of gut microbiota. Polysaccharide treatment notably increased mucin-2 expression, reduced serum cytokine levels (IL-10, TNF-α), and increased tight junction protein production (ZO-1, Occludin, Claudin). Additionally, polysaccharides promoted a significant recovery in gut microbiota composition, indicating potential prebiotic effects. These findings highlight the therapeutic capability of *Anemarrhena asphodeloides* polysaccharides against LTA-induced pneumonia through gut microbiota modulation and restored intestinal homeostasis.

1. Introduction

Pneumonia stands as a prevalent infectious respiratory ailment, characterized by lung inflammation leading to reduced oxygen levels, respiratory distress, and often, fatal outcomes. Statistics from 2011 reveal that approximately 1.2 million children younger than five years old died due to pneumonia, underscoring the devastating effects of the disease. Tragically, the highest incidence of these fatalities is observed in less developed regions, where access to treatment is limited which exacerbates the situation, compounded by insufficient initiatives to enhance care in more affluent nations [1]. Despite the progress made in medical care, pediatric pneumonia continues to be a significant contributor to mortality among infants and young children across the globe. This emphasizes the ongoing challenges in tackling this serious health threat [2,3]. Determining the specific pathogen in pediatric pneumonia is challenging due to the elevated mortality rate linked with the disease. Blood cultures are frequently not very sensitive, and the results of radiography are not specific enough to differentiate between viral and bacterial pneumonia [4].

* Corresponding author.
E-mail address: qjj123wo@126.com (J. Qiu).
[1] These authors contributed equally to this work.

https://doi.org/10.1016/j.heliyon.2024.e39390
Received 28 June 2024; Received in revised form 10 October 2024; Accepted 14 October 2024
Available online 16 October 2024

The lungs and intestines serve as central hubs for a variety of microorganisms [5]. Assessing their flora structure in light of this characteristic provides valuable insights into their interactions [5]. Acting as a closed cavity, the intestine restricts microorganisms from spreading to other tissues while encouraging the proliferation of specific microbial populations [6]. Throughout a prolonged process of co-evolution with humans, intestinal bacteria have developed mechanisms to stimulate adaptive immunity, support nutrient digestion, and absorption, and, unfortunately, play a role in the development of lethal illnesses [7]. *Enterococcus faecalis,* a representative gram-positive coccus, is known for its key virulence factors, such as surface proteins (SPs), secreted lysophosphatidic acid (LTA), and extracellular products (ECPs) [8]. Lipoteichoic acid (LTA), an extensively researched virulence factor, consists of multiple overlapping layers located between the cell wall and membrane of *E. faecalis*. LTA facilitates the induction of pro-inflammatory cytokines, including interleukin (IL)-6 and IL-1β, thereby eliciting a potent inflammatory response [9]. Surface proteins (SPs), which are proteins anchored to the cell wall through covalent attachment to peptidoglycans, are potent immunogenic molecules capable of disrupting both innate and adaptive immune responses in host cells. These SPs are particularly recognizable by the C1 complex, which initiates the classical complement pathway, along with C3-converting enzymes. As a result, this process significantly boosts the presence of neutrophils, macrophages, and natural killer (NK) cells in vivo, effectively triggering organism-specific immune responses [10]. Presently, the primary pathogenic mechanism of bacterial pneumonia involves infection of the respiratory tract, which elevates the inflammatory response within the lungs [11,12]. A study revealed that *Listeria monocytogenes* isolates from the intestines of children with pneumonia administered into the gastrointestinal (GI) tract via gavage, could lead to pulmonary infection. Earlier research has suggested the gut-lung axis theory to explain these interconnected interactions [13].

Although there have been advancements in antimicrobial chemotherapy, pneumococcal pneumonia continues to pose a significant threat to public health, leading to high rates of illness and death. Moreover, the rise and dissemination of multidrug-resistant strains of Streptococcus *pneumoniae* have become a critical concern [14]. Furthermore, *Streptococcus pneumoniae* is the predominant pathogen responsible for lower respiratory tract infections, contributing to the highest number of deaths related to infectious diseases globally [15]. Despite treatment with effective antibiotics, the fatality rate associated with pneumococcal pneumonia remains elevated, ranging from 10 % to 35 % [16]. This underscores the significance of inflammation-induced physiological disruptions in disease progression. Currently, no novel effective treatments for pneumococcal pneumonia have emerged, making vaccination a crucial tool for prevention. Nevertheless, immunocompromised individuals and elderly individuals (aged 65 years and above) remain at elevated risk of potentially fatal pneumococcal pneumonia [17,18]. With globally demographics trending towards an aging population*, Streptococcus pneumoniae* infection is becoming a pressing concern worldwide. The extensive prevalence of pneumococcal pneumonia, coupled with the escalating resistance of *S. pneumoniae* to penicillin and other antimicrobial treatments, underscores the critical necessity for developing effective therapeutic strategies and gaining a more profound insight into its pathogenesis. Moreover, there is interest in exploring the potential of nutritional supplements for preventing *S. pneumoniae* infections as an optimal treatment strategy [19].

Anemarrhena asphodeloides Bunge derived from its dried root. It tastes bitter and has good effects on health. It helps with problems like fever, cough, and constipation. *Anemarrhena* polysaccharides, especially one called *Anemarrhena anemarrhena* polysaccharide (AABP), can help regulate sugar levels, boost the immune system, and fight bacteria. Even small changes in their structure can change how well they work [20]. Previous studies confirm that *Anemarrhena asphodeloides* has a long history in traditional East Asian medicine for thousands of years. Researchers have identified 269 compounds in the plant, including steroidal saponins, flavonoids, and alkaloids. Studies found that its extract has numerous biological activities, such as nervous system effects, anti-tumor, anti-inflammatory effects, antimicrobial antidiabetic, antiviral; and antiaging properties [20].

Despite the extensive pharmacological activities of *Anemarrhena asphodeloides,* its polysaccharides' have not been explored in lipoteichoic acid (LTA)- induced lung inflammation. This study aims to investigate the bioactivities of these polysaccharides in lung inflammation. We hypothesize that polysaccharides from *Anemarrhena asphodeloides* can alleviate LTA-induced lung inflammation and modulate the gut microbiota, providing a potential new therapeutic approach for respiratory conditions associated with bacterial infections.

2. Materials and methods

2.1. Chemicals and reagents

The following materials and reagents were acquired for this study: Brain Heart Infusion broth Medium and Enterococcus Agar medium were sourced from Qingdao Yuanhaibo Biotechnology Co., Ltd.; stool DNA isolation Kit obtained from Chengdu Fuji Biotechnology Co., Ltd.; Trichloroacetic acid procured from Sinopharm Chemical Reagent Company; 2X Taq Plus Master Mix II and HiScript II Q RT super mix for qPCR and 2ChamQ Universal SYBR qPCR Master Mi secured from Nanjing Novozan Biotechnology Co., Ltd.; MUC2 rabbit polyclonal antibody sourced from Wuhan Sanying Biotechnology Co., Ltd.; Occludin, Claudin, and ZO-1 obtained from (proteintech Wuhan China). Ultrasensitive ECL Chemiluminescence Detection Kit acquired from Severn Innovation (Beijing) Biotechnology Co., Ltd. All other reagents used in this study were of analytical grade and obtained from authorized suppliers.

2.2. Preparation of Enterococcus faecium lipoteichoic acid (LTA)

The preparation of lipoteichoic acid (LTA) from pathogenic *Enterococcus faecium* was executed following the methodology used by (33). Briefly, *Enterococcus faecium* strains were retrieved from −80 °C and after the freeze-thaw cycle changed into a liquid state inside the biological safety cabinet under control conditions. After this, the bacterial culture into the brain heart infusion broth medium was inoculated and incubated in a shaker incubator at 37 °C to facilitate growth. Following the culture, the colonies were isolated through

dilution and plating techniques, ensuring the achievement of pure cultures of *Enterococcus faecium* stain. Subsequently, the bacterial cells were exposed to ultrasonic disruption followed by centrifugation to collect supernatant. Following, centrifugation the supernatant was then treated with a 90 % phenol solution, preheated to 65 °C, to facilitate extraction of lipoteichoic acid while eliminating nucleic acid containments. Dialysis was used for purification purposes after extraction. The resultant purified LTA solution underwent freeze drying in a lyophilizer machine, yielding to yellow color powder which indicates the isolated form of LTA from *Enterococcus faecium.* ELISA kit was used to check the quality and integrity of the isolated LTA for further experimental use.

2.3. Polysaccharides extraction

The polysaccharides were extracted from *Anemarrhena asphodeloides* following the method established by Ref. [21] with slight modifications. Polysaccharides were extracted from the dry root of the *Anemarrhena asphodeloides* using a two-step ethanol precipitation method. The dried root was washed, then dried more and ground in a grinder into a fine powder. Subsequently, the dry powder was treated with 95 % ethanol in a constant temperature water bath at 80 °C with a solid-to-liquid ratio of 1:25 to remove the lipids, pigment, and small molecular weight compounds. The resulting mixture was then subjected to centrifugation and the supernatant was collected. Proteins were removed by adding trichloroacetic acid (TCA) to a final concentration of approximately 15 % followed by centrifugation to collect the supernatant. The pH was then adjusted to 7.0 with 1M NaOH. The supernatant was concentrated using a rotary evaporator and 60 % (v/v) of ethanol was added and the mixture was incubated at 4 °C for 24 h. The precipitate was collected and centrifuged, freeze-dried, and designated low molecular weight polysaccharides named (AABP 60). In parallel procedures, a similar extraction was performed but with the final ethanol concentration adjusted to 80 % (v/v), resulting in a high molecular weight polysaccharide (AABP-80).

2.4. Characterization of crude polysaccharide and sugar composition

Monosaccharide compositions were determined by high-performance liquid chromatography (HPLC) after pre-column derivatization. Fifty mg of crude polysaccharide was hydrolyzed with 2 mol/L trifluoroacetic acid at 120 °C for 6 h in a sealed tube. The excess acid was removed by co-distillation with methanol, yielding a dry hydrolysate dissolved in 0.3 mol/L NaOH. A methanol solution of phenyl methoxycarbonyl (PMP) was added, and the mixture was incubated at 70 °C for 1 h. After cooling, the pH was adjusted to neutral, and distilled water was added. The mixture was extracted with chloroform and filtered through a 0.22 μm nylon membrane. The resulting solution (10 μL) was injected into a C18 column connected to a DAD-UV detector. The mobile phase was a mixture of 0.1 mol/L KH2PO4 (pH 10) and acetonitrile (83:17) at a flow rate of 1.0 mL/min and a column temperature of 30 °C. Sugar identification was achieved by comparison with reference monosaccharides, and the molar ratio of monosaccharides was calculated based on peak areas [22]. Additionally, the total sugar content of crude polysaccharides was analyzed using the Phenol-H2SO4 method. A quantity of 50 mg crude polysaccharide was mixed with concentrated sulfuric acid and phenol solution. The mixture was heated to form a colored complex corresponding to the sugars present. The absorbance of the solution was measured at 490 nm using a spectrophotometer, allowing for quantification of individual monosaccharides based on a standard curve prepared with known sugar standards.

2.5. Animal housing and experimental design

Thirty-two, 3-4 weeks-old male BALB/c mice were acquired from the SPF facility of Dalian Medical University, and the use of these animals for experimental purposes was approved by the ethics committee of Dalian Medical University under the approval number "**202310247**. The mice were adapted for one week to a lab environment under germ-free conditions maintained at a standard condition of 22 ± 3 °C and 50 ± 5 % relative humidity, with a 12–12-h light/dark cycle with free access to food and water. Following the acclimatization period, the mice were allocated into four groups using random assignment, ensuring each group (n = 8); (A) Healthy control, model group (B), low-molecular polysaccharides (C), and high-molecular polysaccharides group (D). All, groups except the Healthy control (group A) received an intraperitoneal injection of 5 mg/kg of LTA for 9 days, meanwhile, the Healthy control group received an injection of an equivalent amount of PBS. From day 10th the mice in Group (C&D) low-molecular polysaccharides and high-molecular polysaccharides groups received 400 mg/kg of *Anemarrhena asphodeloides* polysaccharides' respectively for the next 14 days, while the Healthy control and model group received the same amount of PBS for the same duration. On the 24th day of the experiment, all mice were euthanized, and blood and organs were collected for further analysis.

2.6. Disease activity index evaluation

Throughout the experiment, the mice's body weight was recorded each day. Concurrently, close attention was paid to observing their fur condition, respiratory patterns, and incidences of diarrhea.

2.7. Histological examination

Tissue sections of the lungs and colon were harvested after sacrificing the mice and promptly fixed in a 4 % paraformaldehyde solution. After 24 h, the tissue was carefully placed in tissue embedding boxes and fixed on a positively charged slide. Following the fixation step, the tissue section underwent deparaffinization in xylene for 10 min with two changes and a dehydration process by immersion in ethanol solutions of decreasing concentration. For histological examination, H&E staining was carried out as per the

manufacturer's guidelines. Briefly, the tissue section was exposed to hematoxylin solution followed by sequential washing steps, and eosin staining was applied to the tissue section. Following the staining, a reverse sequential immersion in the ethanol solution of increasing concentration was carried out and immersed in xylene for transparency treatment. The slides were then sealed with a mounting medium and observed under the microscope for histological alterations.

2.8. Immunohistochemical analysis of Muc-2

To assess the expression of MUC-2 in colon tissue immunohistochemical analysis was conducted. Initially, the slides were heated at 65 °C for 2 h and then immersed in xylene for deparaffinization. After this, the slides were dehydrated using a decreasing gradient of ethanol concentrations and ultrapure water. Subsequently, antigen retrieval was performed using citrate buffer treatment in a microwave oven, and the tissue secretions were outlined using an oil-based pen to prevent sample loss. The tissue sections were then exposed to endogenous peroxidase blocker for 20 min, and kit reagents were applied following the guidelines provided by the immunohistochemical staining kit (Biotechnologies Biotechnology, based in Beijing, China). The primary antibody anti-mucin-2 antibody, with the dilution (1:2000), was applied and incubated overnight at 4 °C. following incubation with primary antibody the slides were washed with PBS three times each for 10 min and were incubated with biotinylated goat anti-mouse/rabbit IgG polymer. DAP chromogenic solution was then applied to the tissue section for 1–3 min and washed in running tap water for 8 min. Hematoxylin was added and washed again under running tap water. The slides underwent dehydration with ethanol gradient of different concentrations and transparent treatment with xylene. Finally, the slides were mounted and viewed under a microscope to study the labeled immune cells.

2.9. Immunofluorescent staining

To explore the treatment effect of *Anemarrhena asphodeloides* polysaccharides on the expression of Zonula Occludin (ZO-1) protein in the colon of different experimental groups of mice immunofluorescent staining was performed. Initially, the slides were subjected to a 2-h heating process at 65 °C in an incubator, followed by immersion in xylene for deparaffinization. Subsequent dehydration was achieved using a decreasing gradient of ethanol concentrations and ultrapure water. Antigen retrieval was then conducted by treating the tissue section in citrate buffer (pH 6.0) in a microwave oven. After antigen retrieval, the endogenous peroxidase was applied to the tissue sections for 20 min. The primary antibody for ZO-1, diluted at 1:1000, was applied and left to incubate overnight at 4 °C. Subsequently, the slides were washed with PBS and the tissue section was incubated with FITC-labeled fluorescent secondary antibody at room temperature for 1 h. The slides were washed again with PBS and DAPI was added for 5 min to stain the nuclei. After another round of washing the slides were mounted and observed under the microscope.

2.10. Western blot analysis

Protein extraction from colon tissue was carried out using RIPA lysis buffer. The resulting homogenate was subsequently centrifuged to collect the supernatant, which contained the total protein. The protein concentration was determined using a nanodrop machine and the samples were aliquoted and stored at −80 °C for further analysis. For SDS-PAGE electrophoresis, a 10-12 % gel was prepared, and electrophoresis was conducted under steady flow conditions at 30 mA. The SDS page was then transferred to the PVDF membrane and run for 2 h at 212 mA. Following the transfer, the membrane was removed and placed in 5 % skim milk for 2 h at room temperature. The membrane was washed with PBS three times and incubated with primary antibody (claudin-1 1:3000, Occludin 1:3000, GAPDH 1:8000) and incubated overnight at 4 °C. The membrane was washed three times with PBS and then incubated with a secondary antibody at room temperature for 1 h. Following this the membrane underwent another round of washing with PBS. Finally, protein bands were visualized through the application of an enhanced chemiluminescent (ECL) substrate, and subsequent imaging was performed utilizing a gel documentation system.

2.11. Stool DNA extraction and 16S rRNA pyrosequencing

DNA from fecal samples was extracted using a stool DNA isolation kit obtained from Chengdu Fuji Biotechnology Co., Ltd., as per the manufacturer's guidelines provided. DNA quantification was conducted using a Nanodrop machine, and the quality of the samples was assessed by running them on a 1 % agarose gel. The isolated DNA samples were then stored at −80 °C for further use. Subsequently, the V4 region of the 16s rRNA was amplified from the extracted DNA using specific primers 515F (50GTGCCAGCMGCCGCGGTAA-30) and 806R (50-GGACTACHVGGGTWTCTAAT-30). The sample sequencing was performed using the Illumina NovoSeq 600 platform at GUHE info technology Co., Ltd. QIIME software version 1.9.0 was utilized for sequence read processing, adhering to established protocols. Low-quality sequenced data were filtered out based on predefined criteria. Alpha diversity indices, such as richness, Shannon, Simpson, and evenness, were computed using both QIIME and R software. Additionally, beta diversity was evaluated through UniFrac distance metrics, principal coordinate analysis (PCoA), principal component analysis (PCA), and non-metric multidimensional scaling (NMDS). Key biomarkers for each experimental group were identified using LEfSe (linear discriminant analysis effect size). Furthermore, FAPROTAX, Bug Base, and KEGG pathways were employed to analyze metabolites relevant to ecological functions and their roles within prokaryotic clades.

2.12. Measurement of serum cytokines by ELISA

Once mice were euthanized following institutional ethical guidelines, the blood was collected via eye retina puncture. After allowing the blood to coagulate for an hour at room temperature, the serum was extracted by centrifuging the mixture for 15 min at 4 °C at 3500 rpm. The serum was carefully collected and stored at −80 °C for further biochemical analysis. To measure the serum cytokines levels of TNF-α and IL-10, the samples were thawed and processed using an ELISA kit according to manufacturer instructions.

2.13. mRNA expression level in lungs and colon

To measure the expression level of mRNA for IL-10 and TNF-α, lung tissue was harvested and immediately processed for total RNA extraction. The tissue was homogenized in a Triazole reagent. The RNA concentration was then measured using a Nanodrop machine and kept at −80 °C for further analysis. cDNA was synthesized from the extracted RNA using the HiScriptR II Q RT SuperMix for qPCR (Nanjing Novozan Biotechnology Co., Ltd), as per manufacturer instructions. The ChamQ SYBR qPCR MasterMix kit was used to measure the gene expression utilizing Bioer Light Gene 9660 analyzers (Hitech (Beijing) District, Hangzhou, 310053, China). The PCR cycling protocol included an initial incubation at 50 °C for 2 min, followed by a 10-min denaturation step at 95 °C. Subsequently, 40 cycles of PCR were performed with denaturation at 95 °C for 25 s and annealing/extension at 60 °C for 1 min in each. The relative gene expression level was calculated using and evaluated using Gene 9660 system software and GraphPad Prism to compare differences among various experimental groups, GAPDH served as the internal control.

2.14. Statistical analysis

The study employed GraphPad Prism 9.5.1 software for data analysis. To compare data between groups, one-way ANOVA was used, and statistical significance was indicated at a significance level of $P < 0.05$.

3. Results

3.1. Characterization of crude polysaccharide samples

Polysaccharides from *Anemarrhena asphodeloides* were extracted using different concentrations of methanol. The monosaccharide composition and molecular weight of both samples were determined using High-Performance Liquid Chromatography (HPLC) and the phenol-H2SO4 method. The different types and concentrations of monosaccharides present in both the low and high molecular-weight samples are shown in Table 1. HPLC analysis yielded distinct spectra for both samples, revealing varying compositions of compounds and peaks, as illustrated in Fig. 1 A&B.

3.2. Quantification of LTA content in Enterococcus faecium

The content of LTA after extraction from *Enterococcus faecium* was determined using an ELISA assay. The standard curve was constructed with the abscissa representing the standard product concentration and the ordinate representing the corresponding absorbance at 450 nm (A = 450). As shown in Fig. 2 the standard curve regression equation used is:

$y = 5.7194 \times x + 0.0733$ with an $R2R$ 2 value of 0.9949 indicating a strong correlation and precise fitting of the curve. The LTA content was measured by putting the OD value of the LTA solution in a regression equation the concentration was calculated and the purity of the LTA was also calculated using the following formula:

$$\text{Purity} = (\textit{LTA concentration} \times \textit{dilution factor} / \textit{LTA sample solution concentration}) \times 100\%$$

Based on the above calculations, the purity of LTA was determined to be 86.71 %.

Table 1
Monosaccharide composition and molecular weight of low and high molecular weight polysaccharides from *Anemarrhena asphodeloides*.

High molecular polysaccharides			Low Molecular polysaccharides		
Component	Mg/kg	%	Component	Mg/kg	%
Gula	606.29	2.6384	Man	255.21	1.9431
Man	13989.	60.882	Man	7734.97	58.893
Glc	7167.3	31.191	Glc	5143.56	39.162
Gal	1215.0	5.287			
Molecular weight			**Molecular weight**		
Mp (g/mol)	4.42611×10^5	442611	Mp (g/mol)	5.2967×10^4	52967
Mn (g/mol)	2.13326×10^5	213326	Mn (g/mol)	2.4116×10^4	24116
Mw (g/mol)	3.57473×10^5	357473	Mw (g/mol)	5.6879×10^4	56879
Mz (g/mol)	5.21456×10^5	521456	Mz (g/mol)	1.12459×10^5	112459
Mz+1 (g/mol)	6.58422×10^5	658422	Mz+1 (g/mol)	1.57776×10^5	177796

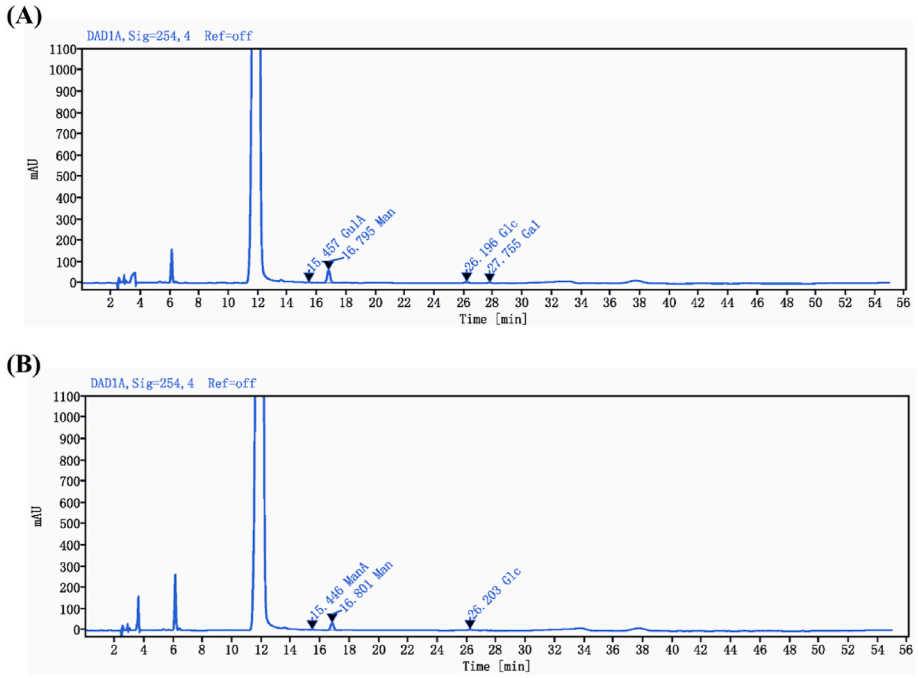

Fig. 1. Chromatogram of Standard Monosaccharide Analysis by HPLC. **(A)** High molecular polysaccharides **(B)** Low molecular Polysaccharides. This chromatogram displays the monosaccharide profiles of polysaccharides analyzed via HPLC. (A) High molecular weight polysaccharides and (B) Low molecular weight polysaccharides are shown, with distinct peaks corresponding to individual monosaccharides. The retention times and peak areas provide insights into the composition and concentration of monosaccharides present in each polysaccharide type.

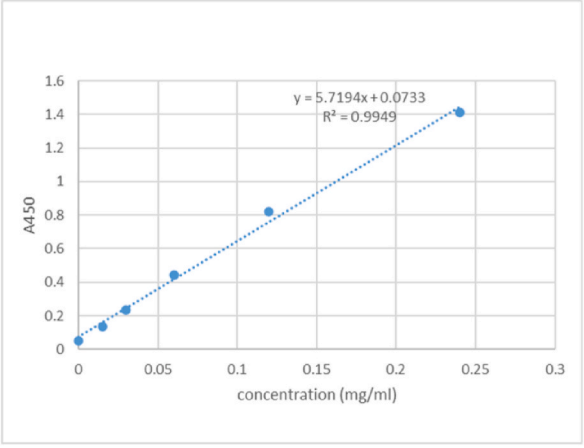

Fig. 2. A standard curve showing the relationship between Lipoteichoic acid (LTA) solution and concentration and absorbance at 450 nm.

3.3. Disease severity evaluation

During the experimental period, after the peritoneal injection of LTA, mice gradually developed symptoms including hair loss, dull fur (Fig. 3A), perianal redness (Fig. 3B and C), and the presence of dark-colored feces as shown in Fig. 3D. Additionally, after sacrificing the mice inflammatory noodles were observed in the colon as shown in Fig. 3E. In contrast mice in the Healthy control exhibited no abnormal symptoms and maintained regular eating and drinking habits. These observations suggest the successful establishment of the LTA-based pneumonia mouse model.

3.4. Histopathological evaluation

H&E staining was used for histological analysis of lung and colon tissue to assess the treatment effect of *Anemarrhena asphodeloides*

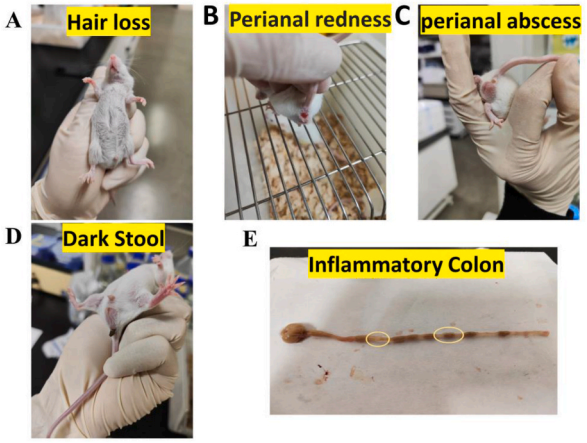

Fig. 3. Disease severity measurement in LTA induces lung inflammation in mice. **(A)** loss and dull fur (**B** and **C**) perianal redness (**D**) the presence of dark-shaped stool (E) inflammatory noodles in the colon.

in LTA-induced lung inflammation mice. The lungs of the normal group exhibited clear alveolar structure with clear air space and an absence of congestion, edema, and inflammatory cells. Conversely, mice in the LTA-treated group showed irregular alveolar structures, extensive infiltration of lymphocytes and macrophages, severe congestion, and varying degrees of pulmonary edema, which show that LTA significantly induced lung inflammation. Nevertheless, upon administration of *Anemarrhena asphodeloides* polysaccharides both the low and high molecular weight polysaccharides significantly reduced the inflammatory cell infiltration, and lung tissue congestion and restored the normal alveolar structure as shown in (Fig. 4A). Additionally, colon tissue was subjected to hematoxylins and Eosin staining for histological examination. The colon in the normal group shows the intact mucus layer, with neatly arranged glands, a clear structure, a normal crypt, a high number of goblet cells, and uniform space with clear borders between the mucosa and submucosa layers. In contrast, the LTA-treated group exhibited irregular mucosal layer, inflammatory masses, partial crypt disappearance, reduced number of goblet cells, intensive villi atrophy, severe tissue damage, and disrupted architecture. Notably, upon *Anemarrhena asphodeloides* polysaccharides supplementation both low and high-molecular weight polysaccharides restored the normal architecture of the colon with clear mucosal and submucosal layers, well-shaped crypts, and a significant increase in the production of goblet cells as depicted in Fig. 4B.

3.5. Immunohistochemical analysis of Muc-2 expression

Mucin-2 is a crucial component of the epithelial barrier in the gut, primarily synthesized and secreted by goblet cells [23].

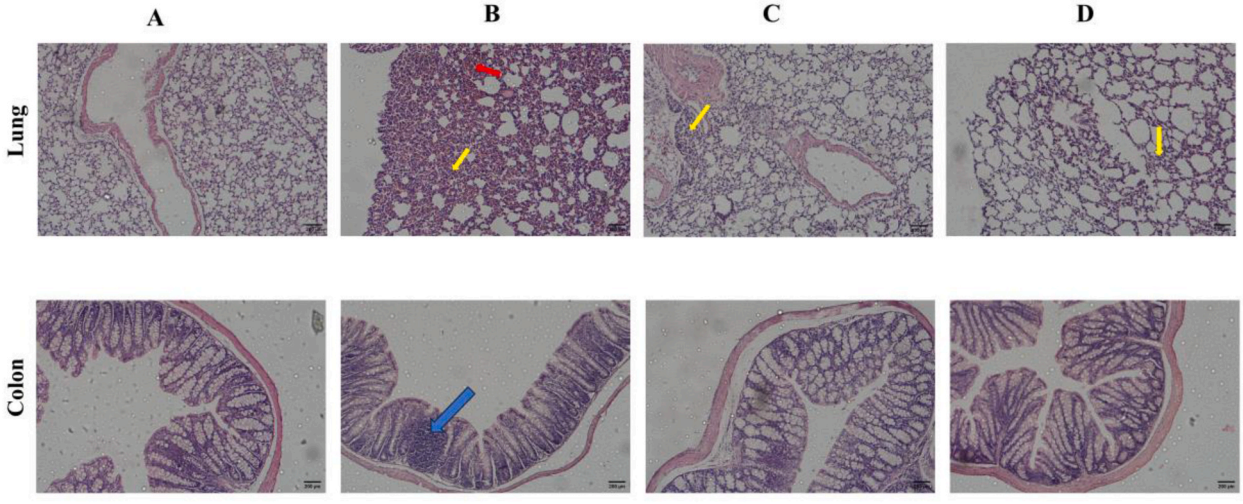

Fig. 4. HE staining, *Anemarrhena asphodeloides* Polysaccharides supplementation alleviates the histopathological alterations. **(A)** *Anemarrhena asphodeloides* Polysaccharides healing effect on lungs. Arrows representing inflammatory cells **(B)** histopathological alteration in the colon, on LTA-induced pneumonia mice, magnification (100x). Groups: (A) Healthy control, (B) LTA model, (C) Low-molecular weight, and (D) High-molecular weight polysaccharides.

Immunohistochemistry staining was performed to assess the therapeutic impact of *Anemarrhena asphodeloides* polysaccharides on the expression of mucin-2 in the context of LTA-induced pneumonia in mice as revealed in Fig. 5. Mice in the Healthy control group exhibited higher mucin expression, while the LTA treated group showed a significant decline in the expression of mucin in the colon tissue of mice ($p < 0.0001$). Following polysaccharide supplementation, low and high-molecular weight polysaccharides raise mucin-2 expression in the colon ($p < 0.01$).

3.6. Serum cytokine levels

Lung infections are influenced by a balance of pro-inflammatory cytokines, such as TNF-α and IL-1β, which promote inflammation, and anti-inflammatory cytokines, including IL-10, TGF-β, and IL-1ra, which are secreted by alveolar macrophages to mitigate the inflammatory response [24]. To assess the treatment effect of *Anemarrhena asphodeloides* on the expression of serum IL-10 and TNF-α levels, they were determined using an ELISA kit in mice of different experimental groups. The expression levels of IL-10 (Fig. 6A) and TNF-α (Fig. 6B) were significantly elevated in the serum of LTA treated group ($p < 0.001$). However, polysaccharide treatment markedly reduced the expression level of these cytokines particularly in high molecular weight polysaccharides ($p < 0.001$), as illustrated in (Fig. 6A and B).

3.7. Anemarrhena asphodeloides polysaccharides enhances the expression of TJS

The structural integrity and barrier function of the intestine is maintained by a group of proteins known as tight junction proteins, which include key components such as zonula occludin-1, claudin-1, and Occludin [25]. These tight junction proteins maintain the integrity of the gut epithelium and the structure of the tight. On the other hand, a decrease in the expression of these proteins leads to an increase in the permeability of the gut epithelium, compromising its barrier function [26,27]. ZO-1 expression in the colon was examined using immunofluorescence labeling. As depicted in Fig. 7 our findings revealed that LTA administration led to a decrease in the expression of ZO-1 as compared to the Healthy control. Nonetheless, polysaccharide treatment with both low and high-molecular-weight polysaccharide groups significantly increased the expression of ZO-1 in the colon tissue of mice as demonstrated in Fig. 7A. To further confirm the expression level of tight junction proteins, the western blotting method was used to evaluate the expression levels of Occludin and Claufin-1 in the colon tissue of mice. Compared to the normal group the LTA-treated group exhibited significantly decreased levels of these proteins ($p < 0.5$). Conversely, polysaccharides treatment, particularly high molecular weight polysaccharides treatment notably upregulated the expression level of these proteins ($p < 0.05$) as shown in Fig. 7B.

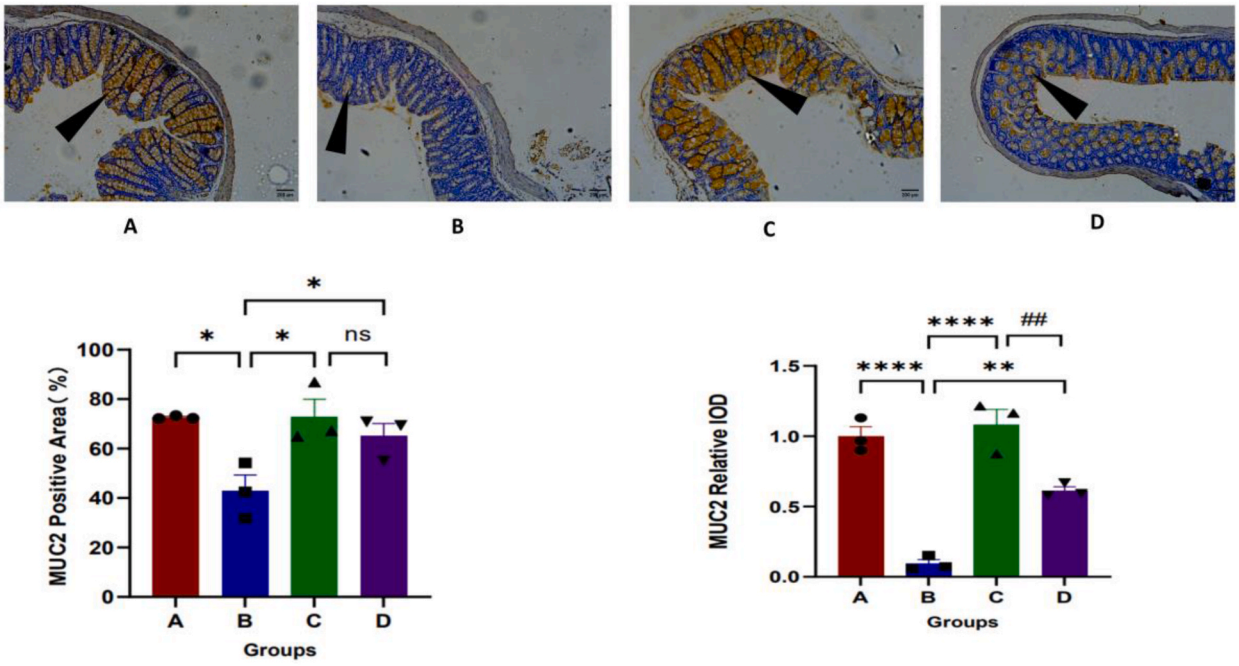

Fig. 5. This analysis shows the upregulation of Mucin-2 in the colon of LTA-induced pneumonia mice treated with *Anemarrhena asphodeloides* polysaccharides. The images illustrate Mucin-2 staining, with a golden-yellow color indicating the presence of Mucin-2. This highlights the protective role of polysaccharides in enhancing mucosal barrier function and suggests potential therapeutic benefits for gut health in this model. Groups: (**A**) Healthy control, (**B**) LTA model, (**C**) Low-molecular weight, and (**D**) High-molecular weight polysaccharides. (For interpretation of the references to color in this figure legend, the reader is referred to the Web version of this article.)

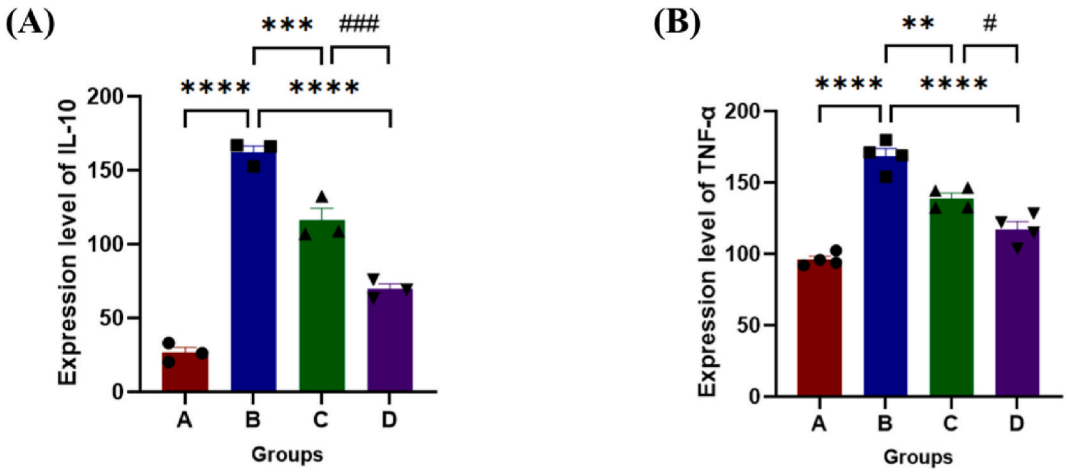

Fig. 6. *Anemarrhena asphodeloides* polysaccharide effect on the Expression Levels of serum cytokines in LTA-induced pneumonia mice **(A)** IL-10 and **(B)** TNF-α in Mice Blood. Groups: (A) Healthy control, (B) LTA model, (C) Low-molecular weight, and (D) High-molecular weight polysaccharides.

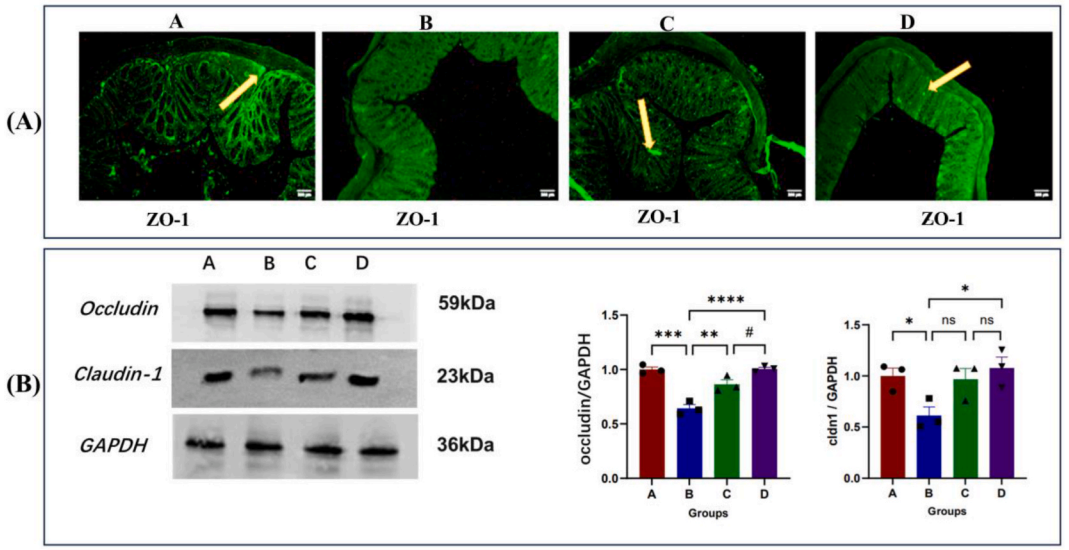

Fig. 7. *Anemarrhena asphodeloides* polysaccharides promote the upregulation of tight junction proteins. (A) Immunofluorescent analysis showing ZO-1 expression in different groups: (A) Healthy control, (B) LTA model, (C) Low-molecular weight polysaccharides, and (D) High-molecular weight polysaccharides. Images highlight the localization and intensity of ZO-1 staining, indicating tight junction integrity. (B) Western blot analysis demonstrating the expression levels of Occludin and Claudin across the groups, revealing the impact of Anemarrhena asphodeloides polysaccharides on tight junction protein regulation.

3.8. Anemarrhena asphodeloides modulate gut microbiota

A range of health conditions, like inflammatory bowel syndrome, colorectal cancer, neurological disorder, inflammatory conditions, and autism spectrum disorder have been reported to cause a decrease in the diversity and complexity of the gut microbiome [28–30]. In this experiment we determined the LTA-induced nominee affects the balance of gut microbiota and also to check the restorative effect of *Anemarrhena asphodeloides* polysaccharides on this dysbiosis. We employed 16S rRNA sequencing to analyze the overall overview and structural characteristics of intestinal microbiota after LTA-induced pneumonia and post-polysaccharides treatment. Upon analyzing the sequenced results the Venn diagram Fig. 8A, shows that the microbial taxa shared between the LTA-treated group and the Healthy control group shared a smaller number of OTU. Conversely, the polysaccharides-treated group exhibited a notably larger overlap in microbial taxa with Healthy control, suggesting that the administration of polysaccharides facilitated a more comprehensive restoration of gut microbiota. These findings suggest the effectiveness of *Anemarrhena asphodeloides* polysaccharides in promoting the recovery of gut microbiota following LTA-induced dysbiosis. Furthermore, alpha diversity

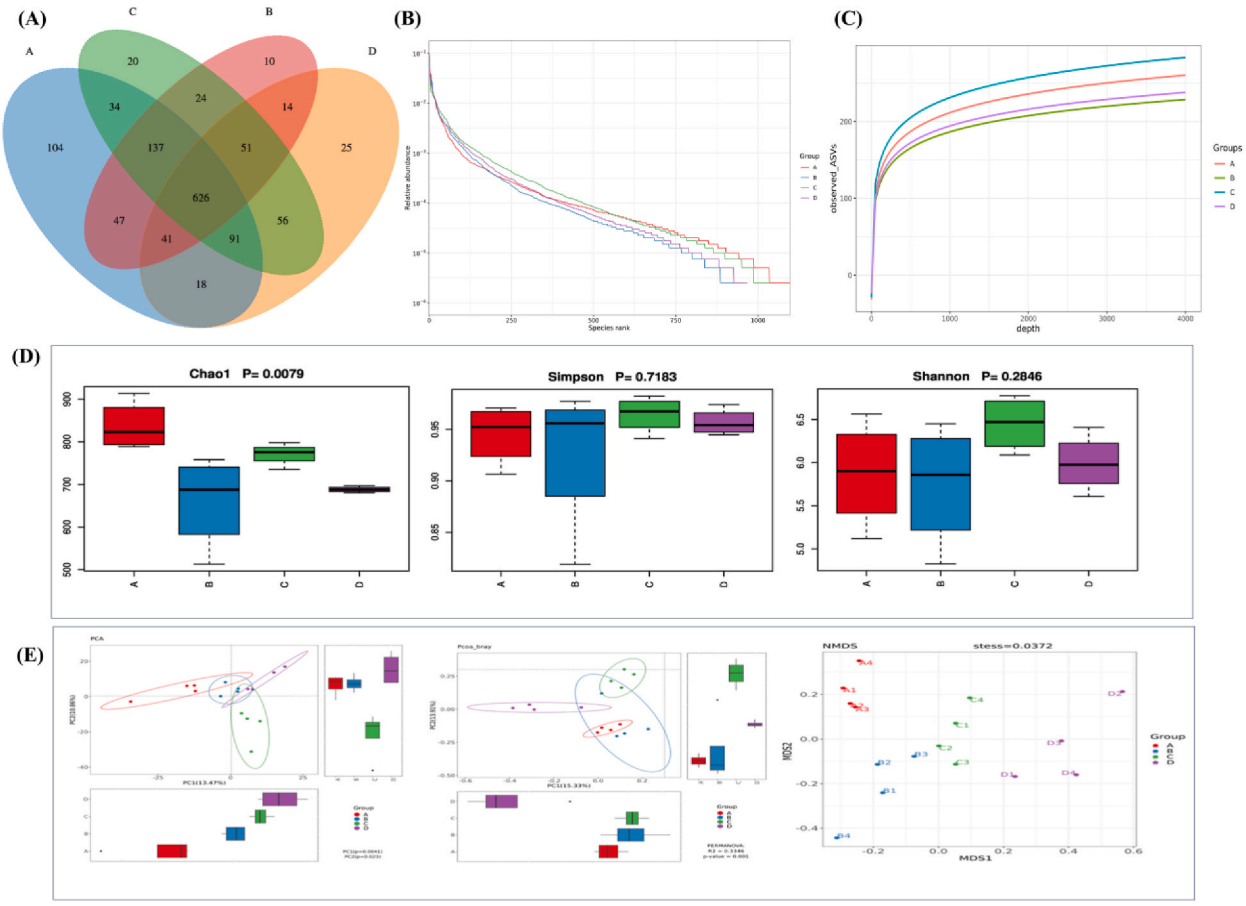

Fig. 8. Alpha and Beta diversity analysis of microbial communities across different experimental groups. (**A**) The Venn diagram shows the shared and unique microbial taxa among the four experimental groups. Overlapping areas represent taxa common between groups, while non-overlapping areas indicate unique taxa. The analysis highlights differences in microbial diversity and shared taxa between the polysaccharide-treated groups and the control and LTA model groups (**B**) Rank abundance curve. This curve shows microbial taxa's relative abundance and evenness across experimental groups. The x-axis represents taxa rank, and the y-axis indicates proportional abundance. Flatter curves reflect greater evenness, highlighting differences in community structure among the control, LTA model, and polysaccharide-treated groups (**C**) Refraction curve, this curve illustrates species richness relative to sampling effort, with the x-axis representing sample size and the y-axis showing observed species. A plateau indicates sufficient sampling, reflecting microbial diversity in the control, LTA model, and polysaccharide-treated groups (**D**) Chao1, Simpson, Shannon, which assess microbial richness and diversity across experimental groups, highlighting the impact of treatments on community structure (**E**) PCA, PCoA, and NMDS, these plots visualize differences in microbial community composition among experimental groups. PCA and PCoA display variation based on similarity metrics, while NMDS emphasizes rank order, highlighting the impact of treatments on microbial diversity. Groups: (A) Healthy control, (B) LTA model, (C) Low-molecular weight, and (D) High-molecular weight polysaccharides.

parameters were evaluated to explore bacterial diversity and richness across different experimental groups. To explore the bacterial richness, a rank abundance curve was utilized. The breadth and shape of the curve represented species richness and abundance. The curve for the Healthy control group (A) was notably extended and broad, signifying a high level of richness. In contrast, the LTA-treated group showed a diminished richness. On the other hand, polysaccharide administration restores this change and increases richness as compared to the LTA group as illustrated in Fig. 8B and C. Furthermore, alpha diversity metrics such as Chao1, Shannon, and Simpson were used to analyze microbial richness and diversity. The chao1 index estimates species richness, while the Simpson index evaluates bacterial diversity. Fig. 8D shows that the Normal group had the highest species abundance, while the LTA-treated group showed a significant decline in the richness ($p < 0.05$). The low molecular weight polysaccharides show the highest ranches of bacterial diversity followed by a higher molecular weight polysaccharides group.

Moreover, beta diversity parameters such as Principal component analysis (PCA), Principal coordinate Analysis (PCoA), and non-metric Multidimensional Scaling (NMDS) were utilized to explore the similarity in sample community compositions. Our results show significant distinction between the LTA-treated group and the Healthy control group. The sample structure of the LTA group was found significantly different from that of the Healthy control, while the polysaccharide group restored all these parameters and showed its prebiotic effect, as shown in Fig. 8E.

To further explore the prebiotic effect of *Anemarrhena asphodeloides* polysaccharides on LTA-induced dysbiosis the species

composition at phylum and family level were evaluated. Fig. 9A shows that in the model group, a notable increase in the abundance of Bacteroidetes and Campylobacteria was observed, while firmicutes richness was significantly reduced in the LTA-treated group as compared to the Healthy control group. However, following polysaccharides treatment, both molecular weight polysaccharides exhibited a notable decrease in the richness of Bacteroidetes and Campylobacteria, accompanied by an increase in Firmicutes level, resembling those observed in the Healthy control group. Particularly the low molecular weight polysaccharides showed a significant increase in the firmicutes. Fig. 9B presents the top three families identified among all four experimental groups. Notable families observed include *Muribaculaceae*, *Bacteroidota*, *Lactobacillaceae*, and *Lachnospiraceae.* Results revealed that, compared to the Healthy control group the LTA group exhibited an elevated abundance of *Muribaculaceae* and *Lachnospiraceae*, while the levels of *Lactobacillaceae* and *Rikenellaceae* decreased. After polysaccharide treatment, the low molecular weight polysaccharides show a decline in *Muribaculaceae,* accompanied by an increase in *Lactobacillaceae*, *Lachnospiraceae*, and *Rikenellaceae*. High molecular weight polysaccharide was observed with a reduction in the abundance of *Muribaculaceae* and *Rikenellaceae,* while the *Lactobacillaceae* and *Prevotellaceae* were found to be increased as shown in Fig. 9C.

Furthermore, Bug Base analysis was used to distinct the prevalence of different phenotypes, including forming biofilms, potentially pathogenic, aerobic and anaerobic, and stress-tolerant strains among all groups as shown in Fig. 9D. The LTA group exhibited the highest number of Gran-negative bacteria, the poorest tolerance to oxidative stress, the highest potential for pathogenic bacteria and a smaller number of Gram-positive bacteria. In contrast, both the low and high-molecular weight group demonstrated the opposite of the LTA group and restored all the changes caused by LTA.

Moreover, Discriminant Analysis Effect Size (LEfSe) was used to determine the taxonomy biomarkers. Results revealed that the Healthy control group, the *Eggerthellaceae, Coriobacteriales, Anaerovoracaceae,* and *Peptostreptococales_tissierell* are the dominant taxa. The normal group shows a decline in these all taxa and is found to increase in the *Gamma proteobacteria* and *Defluviitaleaceae.* Following polysaccharide treatment, the low-dose polysaccharide group exhibits *Marinifilaceae, Acholeplasmataceae,* and *Lachnospiraceae* as dominant biomarkers as illustrated in Fig. 10A. These results suggest that both low and high molecular weight of polysaccharide treatment may help to restore intestinal dysbiosis by adjusting the relative abundance of specific bacterial groups, potentially counteracting the disruptions in the LTA treated Group. Furthermore, to explore the prebiotic effect of the polysaccharide on energy metabolism, KEGG pathways were utilized. Results exhibited a difference between the LTA-treated group and the control group. The pathways exhibiting the highest enrichment include sulfate and nitrogen respiration, amino acid biosynthesis and metabolism, starch and creatinine degradation, energy production, and sucrose biosynthesis, as demonstrated in Fig. 10B. These alterations suggest that polysaccharide supplementation enhances energy metabolism by modulating the gut microbiota.

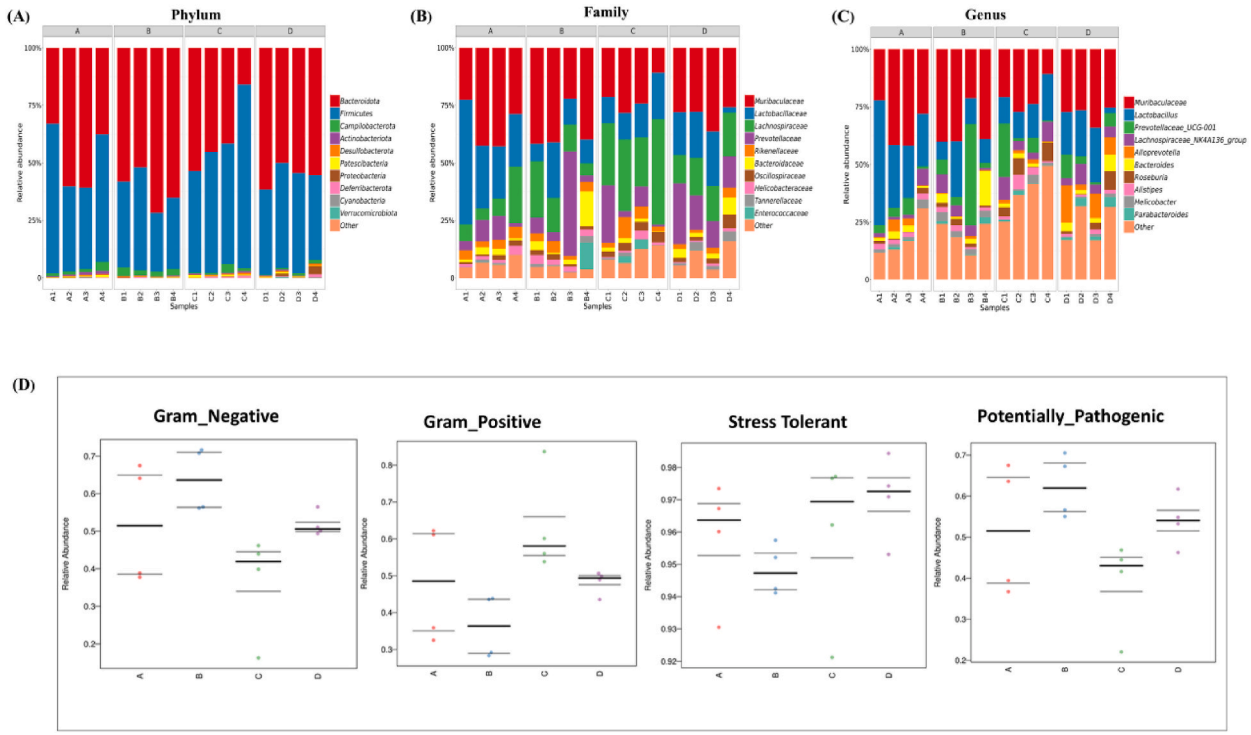

Fig. 9. Taxonomic analysis explores the prebiotic effect of *Anemarrhena asphodeloides* polysaccharides in the context of LTA-induced Dysbiosis**. (A)** phylum level **(B)** Family level **(C)** Genus level **(D)** Bug-Based Analysis of Microbial Phenotypes, this analysis categorizes microbial taxa based on Gram-negative and Gram-positive characteristics, stress tolerance, and pathogenic potential. The results illustrate the distribution of other phenotypes across experimental groups, highlighting variations in community composition and the prevalence of stress-tolerant and potentially pathogenic bacteria. Groups: (A) Healthy control, (B) LTA model, (C) Low-molecular weight, and (D) High-molecular weight polysaccharides.

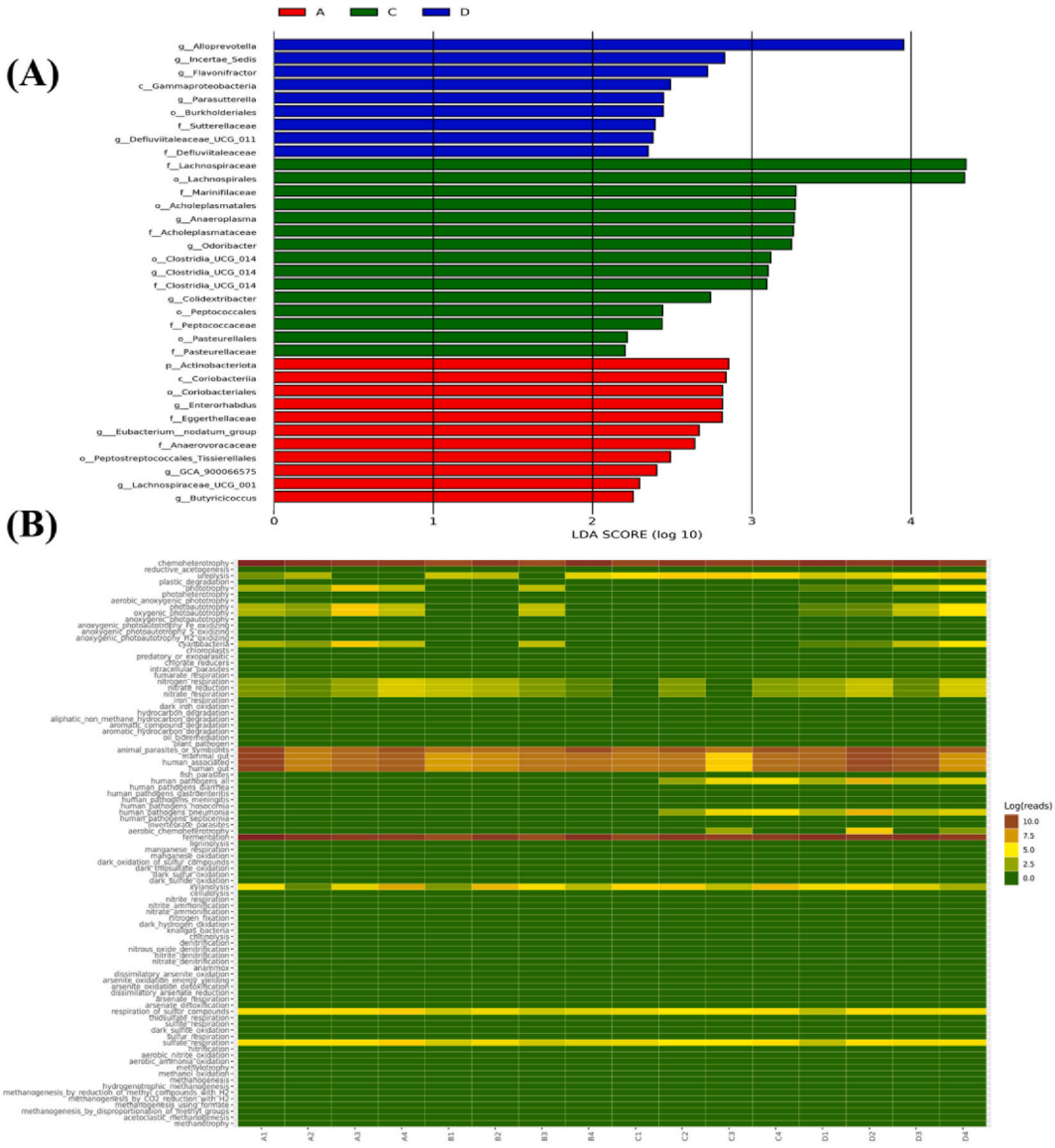

Fig. 10. Effect of *Anemarrhena asphodeloides* Polysaccharides on Gut Dysbiosis. **(A)** Heatmap analysis illustrating the relative abundance of various bacterial taxa across experimental groups: (**A**) Healthy control, (**B**) LTA model, (**C**) Low-molecular-weight polysaccharides, and (**D**) High-molecular weight polysaccharides. The color gradient indicates differences in abundance, with darker shades representing higher levels of specific taxa. (**B**) LEfSe analysis identifying significantly differentially abundant bacterial taxa among the groups, providing insights into the impact of Anemarrhena asphodeloides polysaccharides on gut microbiota composition. (For interpretation of the references to color in this figure legend, the reader is referred to the Web version of this article.)

4. Discussion

Lower respiratory infections, including pneumonia, are a leading cause of morbidity and mortality worldwide, accounting for a substantial proportion of the global disease burden [31]. Pneumonia deaths are higher in less developed regions due to limited access to treatment. This is made worse by inadequate healthcare initiatives in wealthier nations. Globally, half of the population lacks access to essential health services, and 100 million people are pushed into poverty due to healthcare costs [32]. Existing research has predominately focused on respiratory tract infections. These studies have established that lung disease can stem from disruptions in intestinal function and an imbalance in the gut microbiota, thereby substantiating the gut-lung axis hypothesis [33,34]. The intestine, long regarded as the primary digestive site, contains over 70 % of the body's immune cells within its mucosal layer [35,36]. The lungs and intestines serve as central hubs for a variety of microorganisms [5]. This study demonstrates the therapeutic potential of low and high-molecular weight polysaccharides derived from *Anemarrhena asphodeloides* in treating lipoteichoic acid (LTA)-induced pneumonia. The polysaccharides effectively alleviate lung and colon inflammation, restore gut microbiota balance, and enhance mucin-2

expression and tight junction protein production. Additionally, the treatment reduces serum cytokine levels, indicating a significant impact on both respiratory and intestinal health. These findings suggest that *Anemarrhena asphodeloides* polysaccharides may offer a promising therapeutic approach for bacterial-induced lung inflammation through modulation of gut microbiota and restoration of intestinal homeostasis.

The biological activity of biopolymers is influenced by their structural characteristics, including molecular weight, degree of sulfation, sugar composition, and glycosidic branching patterns [37,38]. It is well established that low-molecular-weight (LMW) polysaccharides tend to exhibit higher biological activity compared to high-molecular-weight (HMW) polysaccharides. For instance, sulfated dextrans with molecular weights in the range of 10–500 kDa have demonstrated enhanced anti-HIV activity, while polysaccharides within the 100–200 kDa range have been shown to exhibit strong antitumor effects. Conversely, polymers with molecular weights of 5–10 kDa often lack significant biological activity [39]. Interestingly, polymers around 10 kDa still show strong antiviral properties, particularly in anti-HIV activity [40]. Consistent with these findings, our study demonstrates that LMW polysaccharides exhibit significant therapeutic effects. Specifically, our results indicate that LMW polysaccharides effectively attenuate LTA-induced lung inflammation by modulating gut microbiota composition and reducing inflammatory markers. This is in line with previous research indicating that LMW polysaccharides are more effective at enhancing immunity and exerting antiviral activities compared to their HMW counterparts [40]. Furthermore, our findings reinforce the importance of molecular weight in determining the biological activity of polysaccharides. LMW polysaccharides appear to be more efficient in modulating immune responses and mitigating inflammation, a characteristic that makes them particularly useful in treating LTA-induced inflammatory conditions.

In the current study, we used pathogenic *Enterococcus faecium* to extract Lipoteichoic acid and use it for the development of LTA-induced pneumonia. The mice received 5 mg/kg of lipoteichoic acid for 9 consecutive days to induce a mouse model of pneumonia. Studies found that uncovered fur, dull eyes, and difficulty breathing are symptoms commonly associated with pneumonia in mice [41]. Similar results were found during the experimental period, after the LTA administrations, mice gradually developed symptoms including hair loss, dull fur, perianal redness, and dark-shaped feces. The colon was found to have inflammatory nodules were observed.

The infection triggers not just an inflammatory reaction but also activates the coagulation system, which is regarded as the host's effort to contain the bacterial spread and localize the inflammatory response [42]. The involvement of local coagulation system activation has been linked to the development of bacterial pneumonia [43,44]. In our study, histological analysis showed that LTA induced significant lung inflammation, characterized by irregular alveolar structures, inflammatory cell infiltration, and congestion. Treatment with *Anemarrhena asphodeloides* polysaccharides restored all these histological alterations. Similar results were reported by Refs. [45,46] indicating consistency with our results.

Mucin-2 serves as a pivotal component of the gut epithelial barrier, predominantly synthesized by goblet cells [47]. In the current study, IHC was carried out to investigate the expression of mucin-2 in mice colon tissue. Results revealed that LTA administration for 9 days led to mucin depletion as compared to the Healthy control group. On the other hand, post-LTA treatment with polysaccharides increases the expression of mucin-2 in the colon. Our findings are supported by previously published work conducted by Ref. [48].

Circulating soluble microbial components and metabolites interact with intestinal microorganisms and the lungs, potentially harming intestinal barrier function. This can lead to the leakage of LPS, peptidoglycan, and inflammatory mediators into the circulation system from the intestine, triggering an inflammatory response [49]. Moreover, previously published work reported that endotoxin-induced mild and temporary lung injury which leads to inflammation [50]. Conditions like intestinal injury and inflammation are known to increase the expression of pro-inflammatory cytokines within the intestine [51,52]. At the same time, in our study, we used LTA to induce lung inflammation, and results indicate a significant increase in serum IL-10 and TNF-α levels in the LTA group. However, *Anemarrhena asphodeloides* polysaccharide supplementation reduced the expression of these cytokines. Our results are supported by previously published work by Ref. [53] the used polysaccharide from the lignified okra.

Tight junction proteins play a crucial role in preserving structure integrity and the intestinal barrier function. Key protein in this group includes Occludin, zonula occludens-1, and claudin [25,54]. These junctions' proteins are responsible for preserving the integrity, structure, and function of the barrier junctions [26,27,55]. Immunofluorescent staining and western blotting were used to determine the expression of the tight junction protein. Our results indicate that LTA administration for 9 days connectively leads to a decrease in the expression of these tight junction proteins. However, treatment with *Anemarrhena asphodeloides* polysaccharide reverses the normal expression of tight junction protein. Our findings are in alignment with prior research by Ref. [48] who explored the treatment effect of polysaccharides isolated from *Dictyophora indusiate to* improve gut health and increase intestinal barrier function via increasing the expression of tight junction protein.

Reduced bacterial diversity and richness of intestinal microbiota have been associated with various medical deconditions, including inflammatory bowel disease, neurological and inflammatory disorder, colorectal cancer, and autism [28,29,56]. A previously published study by Ref. [41] show that LTA administration can lead to disruption of gut microflora. Their results further discovered that bacterial richness and diversity were noticeably decreased in *E. faecalis*-extracted LTA group. Additionally, they reported the increase of pathogenic bacteria that released endotoxin and a decline in the reduction of lactobacillus and firmicutes. Simultaneously, our finding revealed an increased abundance of Bacteroides and proteobacteria in the LTA-treated group at the phylum level, also the firmicutes and lactobacillus were decreased with LTA administration, while the polysaccharides supplementation reversed this LTA-induced dysbiosis. While this study provides valuable insights into the distinct effects of low and high-molecular-weight polysaccharides, there are some limitations that should be acknowledged. One notable limitation is the absence of detailed mechanistic insights at the molecular level to fully explain these effects. Additionally, the use of an animal model may not entirely reflect the complexity of human disease. Future research should focus on identifying the precise molecular pathways through which these polysaccharides exert their therapeutic effects, while also exploring potential synergistic interactions with other bioactive

compounds to enhance their efficacy.

5. Conclusion

In conclusion, our comprehensive analysis, encompassing biochemical, histological, and 16S rRNA sequencing data, demonstrates that administration of *Enterococcus faecalis* lipoteichoic acid (LTA) induced symptoms in mice including hair loss, dull fur, perianal abscess, and dark-shaped stool, as well as irregular alveolar structures, inflammatory cell infiltration and congestion. LTA also disrupts gut microbiota, leading to gut barrier injury, increased expression of proinflammatory cytokines, and decreased levels of mucin and tight junction proteins in the intestines. Furthermore, our analysis indicates that LTA reduced bacterial richness and diversity while increasing pathogenic bacteria. Conversely, supplementation with *Anemarrhena asphodeloides* polysaccharides mitigated LTA-induced dysbiosis, restoring levels of beneficial bacteria such as firmicutes and lactobacillus, enhancing mucin production, increasing tight junction proteins, and decreasing the production of proinflammatory cytokines. Overall, these results suggest that *Anemarrhena asphodeloides* polysaccharides hold promise as a medicinal intervention for bacterial pneumonia, potentially mitigating inflammation and restoring intestinal homeostasis.

CRediT authorship contribution statement

Yuqi Wen: Methodology. **Hidayat Ullah:** Writing – original draft, Investigation. **Renzhen Ma:** Methodology. **Nabeel Ahmad Farooqui:** Methodology. **Jiaxin Li:** Methodology. **Yamina Alioui:** Methodology. **Juanjuan Qiu:** Writing – review & editing, Supervision, Investigation, Funding acquisition, Conceptualization.

Institutional review ethical board statement

This study was approved by the Dalian Medical University Committee for Animal Experiments, and animal handling adhered to the guidelines on the Care and Use of Laboratory Animals set forth by the National Institutes of Health.

Data availability statement

The original data for this work is available upon email request to the corresponding author.

Funding

National Nature Science Foundation of China (Grant No.81803896). The role of the funder is to provide funding for the experiment.

Declaration of competing interest

The authors declare that they have no known competing financial interests or personal relationships that could have appeared to influence the work reported in this paper.

Appendix A. Supplementary data

Supplementary data to this article can be found online at https://doi.org/10.1016/j.heliyon.2024.e39390.

References

[1] C. von Mollendorf, et al., Aetiology of childhood pneumonia in low-and middle-income countries in the era of vaccination: a systematic review, Journal of global health 12 (2022).
[2] J.M. Langley, J.S. Bradley, Defining pneumonia in critically ill infants and children, Pediatr. Crit. Care Med. 6 (3) (2005) S9–S13.
[3] D.A. McAllister, et al., Global, regional, and national estimates of pneumonia morbidity and mortality in children younger than 5 years between 2000 and 2015: a systematic analysis, Lancet Global Health 7 (1) (2019) e47–e57.
[4] S.K. Obaro, S.A. Madhi, Bacterial pneumonia vaccines and childhood pneumonia: are we winning, refining, or redefining? Lancet Infect. Dis. 6 (3) (2006) 150–161.
[5] L. Cuthbertson, et al., Lung function and microbiota diversity in cystic fibrosis, Microbiome 8 (2020) 1–13.
[6] S. Sivaprakasam, et al., Cell-surface and nuclear receptors in the colon as targets for bacterial metabolites and its relevance to colon health, Nutrients 9 (8) (2017) 856.
[7] S. Gude, et al., Bacterial coexistence driven by motility and spatial competition, Nature 578 (7796) (2020) 588–592.
[8] P. Lüthje, A. Brauner, Virulence factors of uropathogenic E. coli and their interaction with the host, Adv. Microb. Physiol. 65 (2014) 337–372.
[9] G. Erbs, M.A. Newman, The role of lipopolysaccharide and peptidoglycan, two glycosylated bacterial microbe-associated molecular patterns (MAMPs), in plant innate immunity, Mol. Plant Pathol. 13 (1) (2012) 95–104.
[10] T.J. Foster, et al., Adhesion, invasion and evasion: the many functions of the surface proteins of Staphylococcus aureus, Nat. Rev. Microbiol. 12 (1) (2014) 49–62.
[11] R.M. Zash, et al., The aetiology of diarrhoea, pneumonia and respiratory colonization of HIV-exposed infants randomized to breast-or formula-feeding, Paediatr. Int. Child Health 36 (3) (2016) 189–197.

[12] L. Palmer, et al., Respiratory outcomes, utilization and costs 12 months following a respiratory syncytial virus diagnosis among commercially insured late-preterm infants, Curr. Med. Res. Opin. 27 (2) (2011) 403–412.
[13] N. Hernando, et al., Intestinal depletion of NaPi-IIb/slc34 a2 in mice: renal and hormonal adaptation, J. Bone Miner. Res. 30 (10) (2015) 1925–1937.
[14] P. Singh, J. Holmen, Multidrug-resistant infections in the developing world, Pediatric Clinics 69 (1) (2022) 141–152.
[15] J.J. Park, et al., Estimating the global and regional burden of Streptococcus pneumoniae meningitis in children: protocol for a systematic review and meta-analysis, JMIR Research Protocols 13 (1) (2024) e50678.
[16] P. Naucler, et al., Contribution of host, bacterial factors and antibiotic treatment to mortality in adult patients with bacteraemic pneumococcal pneumonia, Thorax 68 (6) (2013) 571–579.
[17] M. Cabre, Pneumonia in the elderly, Curr. Opin. Pulm. Med. 15 (3) (2009) 223–229.
[18] V. Kaplan, et al., Hospitalized community-acquired pneumonia in the elderly: age-and sex-related patterns of care and outcome in the United States, Am. J. Respir. Crit. Care Med. 165 (6) (2002) 766–772.
[19] T. Okimura, et al., Therapeutic effects of an orally administered edible seaweed-derived polysaccharide preparation, ascophyllan HS, on a Streptococcus pneumoniae infection mouse model, Int. J. Biol. Macromol. 154 (2020) 1116–1122.
[20] C. Liu, et al., A review of the botany, ethnopharmacology, phytochemistry, pharmacology, toxicology and quality of Anemarrhena asphodeloides Bunge, J. Ethnopharmacol. 302 (2023) 115857.
[21] N. Wang, et al., Antioxidant property of water-soluble polysaccharides from Poria cocos Wolf using different extraction methods, Int. J. Biol. Macromol. 83 (2016) 103–110.
[22] L. Hao, et al., Characterization and antioxidant activities of extracellular and intracellular polysaccharides from Fomitopsis pinicola, Carbohydr. Polym. 141 (2016) 54–59.
[23] M.S.d.A. Yamashita, E.O. Melo, Mucin 2 (MUC2) promoter characterization: an overview, Cell Tissue Res. 374 (3) (2018) 455–463.
[24] B. Moldoveanu, et al., Inflammatory mechanisms in the lung, J. Inflamm. Res. (2008) 1–11.
[25] R. Noth, et al., Increased intestinal permeability and tight junction disruption by altered expression and localization of occludin in a murine graft versus host disease model, BMC Gastroenterol. 11 (2011) 1–9.
[26] A.S. Fanning, et al., The tight junction protein ZO-1 establishes a link between the transmembrane protein occludin and the actin cytoskeleton, J. Biol. Chem. 273 (45) (1998) 29745–29753.
[27] J. Zhao, et al., A protease inhibitor against acute stress-induced visceral hypersensitivity and paracellular permeability in rats, Eur. J. Pharmacol. 654 (3) (2011) 289–294.
[28] J. Ahn, et al., Human gut microbiome and risk for colorectal cancer, J. Natl. Cancer Inst. 105 (24) (2013) 1907–1911.
[29] I.M. Carroll, et al., Alterations in composition and diversity of the intestinal microbiota in patients with diarrhea-predominant irritable bowel syndrome, Neuro Gastroenterol. Motil. 24 (6) (2012), 521-e248.
[30] H. Ullah, et al., Polysaccharides derived from Deglet Noor dates modulate amoxicillin-induced dysbiosis and enhance intestinal barrier function, J. Funct.Foods 120 (2024) 106350.
[31] C. Troeger, et al., Estimates of the global, regional, and national morbidity, mortality, and aetiologies of lower respiratory infections in 195 countries, 1990–2016: a systematic analysis for the Global Burden of Disease Study 2016, Lancet Infect. Dis. 18 (11) (2018) 1191–1210.
[32] W.H. Organization, Tracking Universal Health Coverage: 2023 Global Monitoring Report, World Health Organization, 2023.
[33] H.K. Eslamy, B. Newman, Pneumonia in normal and immunocompromised children: an overview and update, Radiol. Clin. 49 (5) (2011) 895–920.
[34] J. Tang, et al., Effect of gut microbiota on LPS-induced acute lung injury by regulating the TLR4/NF-kB signaling pathway, Int. Immunopharm. 91 (2021) 107272.
[35] C. Dejea, E. Wick, C.L. Sears, Bacterial oncogenesis in the colon, Future Microbiol. 8 (4) (2013) 445–460.
[36] W.R. Russell, et al., Colonic bacterial metabolites and human health, Curr. Opin. Microbiol. 16 (3) (2013) 246–254.
[37] H. Qi, et al., Antioxidant activity of different sulfate content derivatives of polysaccharide extracted from Ulva pertusa (Chlorophyta) in vitro, Int. J. Biol. Macromol. 37 (4) (2005) 195–199.
[38] Q. Zhang, et al., Antioxidant activities of sulfated polysaccharide fractions from Porphyra haitanesis, J. Appl. Phycol. 15 (2003) 305–310.
[39] L. Sun, et al., Preparation of different molecular weight polysaccharides from Porphyridium cruentum and their antioxidant activities, Int. J. Biol. Macromol. 45 (1) (2009) 42–47.
[40] C. Haslin, et al., In vitro anti-HIV activity of sulfated cell-wall polysaccharides from gametic, carposporic and tetrasporic stages of the Mediterranean red alga Asparagopsis armata, Planta Med. 67 (4) (2001) 301–305.
[41] Z. Tian, et al., Mechanisms of lung and intestinal microbiota and innate immune changes caused by pathogenic Enterococcus faecalis promoting the development of pediatric pneumonia, Microorganisms 11 (9) (2023) 2203.
[42] S.M. Opal, Phylogenetic and functional relationships between coagulation and the innate immune response, Crit. Care Med. 28 (9) (2000) S77–S80.
[43] M. Levi, et al., Bronchoalveolar coagulation and fibrinolysis in endotoxemia and pneumonia, Crit. Care Med. 31 (4) (2003) S238–S242.
[44] M.J. Schultz, et al., Pulmonary coagulopathy as a new target in therapeutic studies of acute lung injury or pneumonia—a review, Crit. Care Med. 34 (3) (2006) 871–877.
[45] A.W. Rijneveld, et al., Plasminogen activator inhibitor type–1 deficiency does not influence the outcome of murine pneumococcal pneumonia, Blood 102 (3) (2003) 934–939.
[46] A.W. Rijneveld, et al., Local activation of the tissue factor-factor VIIa pathway in patients with pneumonia and the effect of inhibition of this pathway in murine pneumococcal pneumonia, Crit. Care Med. 34 (6) (2006) 1725–1730.
[47] M. Van der Sluis, et al., Muc2-deficient mice spontaneously develop colitis, indicating that MUC2 is critical for colonic protection, Gastroenterology 131 (1) (2006) 117–129.
[48] S. Kanwal, et al., A polysaccharide isolated from Dictyophora indusiata promotes recovery from antibiotic-driven intestinal dysbiosis and improves gut epithelial barrier function in a mouse model, Nutrients 10 (8) (2018) 1003.
[49] R.M. Logan, et al., The role of pro-inflammatory cytokines in cancer treatment-induced alimentary tract mucositis: pathobiology, animal models and cytotoxic drugs, Cancer Treat Rev. 33 (5) (2007) 448–460.
[50] K. Kabir, et al., Characterization of a murine model of endotoxin-induced acute lung injury, Shock 17 (4) (2002) 300–303.
[51] Y. Liu, et al., Dietary arginine supplementation alleviates intestinal mucosal disruption induced by Escherichia coli lipopolysaccharide in weaned pigs, Br. J. Nutr. 100 (3) (2008) 552–560.
[52] J. Lallès, et al., Weaning is associated with an upregulation of expression of inflammatory cytokines in the intestine of piglets, J. Nutr. 134 (3) (2004) 641–647.
[53] Y. Liu, et al., Structural characterization and anti-inflammatory activity of a polysaccharide from the lignified okra, Carbohydr. Polym. 265 (2021) 118081.
[54] C. Förster, Tight junctions and the modulation of barrier function in disease, Histochem. Cell Biol. 130 (2008) 55–70.
[55] L. Shen, et al., Tight junction pore and leak pathways: a dynamic duo, Annu. Rev. Physiol. 73 (2011) 283–309.
[56] K. Matsuoka, T. Kanai, The gut microbiota and inflammatory bowel disease, in: Seminars in Immunopathology, Springer, 2015.